Mathematical Modelling of Unmanned Aerial Vehicles

SAEED SARWAR*, SAEED-UR-REHMAN*, AND SYED FEROZ SHAH**

RECEIVED ON 31.12.2012 ACCEPTED ON 05.06.2013

ABSTRACT

UAVs (Unmanned Arial Vehicleis) UAVs are emerging as requirement of time and it is expected that in next five to ten years, complete air space will be flooded with UAVs, committed in varied assignments ranging from military, scientific and commercial usage. Non availability of human pilot inside UAV necessitates the requirement of an onboard autopilot in order to maintain desired flight profile against any unexpected disturbance and/or parameter variations. Design of such an autopilot requires an accurate mathematical model of UAV. The aim of this paper is to present a consolidated picture of UAV model. This paper first consolidates complete 6 DOF Degree of Freedom) equations of motion into a nonlinear mathematical model and its simulation using model parameters of a real UAV. Model is then linearized into longitudinal and lateral modes. State space models of linearized modes are simulated and analyzed for stability parameters. The developed model can be used to design autopilot for UAV.

Key Words: **Unmanned Aerial Vehicles, Mathematical Modeling, Stability Analysis of UAVs, Aerodynamic Parameters of UAV.**

1. INTRODUCTION

In recent yearsUAVs have attracted increasing interest from Defense as well as commercial sector. The significant advantages of UAVs include no risk to human life and lesser operational cost as compared to manned aircrafts.

Majority of UAVs being developed today are used for the missions like reconnaissance, surveillance, search & rescue, border patrolling, anti-drug trafficking, route monitoring, etc. All such tasks can be successfully completed by conducting a low to medium maneuverability flight at relatively low altitudes.

In order to make a UAV fly according to a desired flight profile, control effort in the form of AFCS (Automatic Flight Control System) is required. Linear control theory, nonlinear and intelligent control techniques are being used for the design of UAV controllers. The selection of a particular control technique generally depends upon the category of UAV and its mission requirements.

In order to develop a control system, availability of a realistic mathematical model of a UAV is of paramount importance. The model should include the essential characteristics of the underlying physical system. In-depth

* Centre for Advanced Studies in Engineering (CASE), Islamabad
** Assistant Professor, Department of Basic Sciences & Related Studies, Mehran University of Engineering & Technology, Jamshoro.

understanding of various physical phenomena and respective governing laws is also essential in order to make realistic assumptions and simplifications in the derived equations of mathematical model.

A mathematical model is a set of differential equations describing the characteristics of a system. In case of aircrafts or UAVs the differential equations depicting the dynamic behavior, also referred to as EoM (Equations of Motion), can be expressed in several forms, i.e. as Non-linear Fully-coupled, Non-linear Semi-coupled, Non-linear decoupled, Linear coupled, and Linear decoupled [1] forms. Non-linear Fully-coupled models describe the UAV dynamics more accurately than any other simplified models and are mostly used for evaluating aircraft performance through computer simulations. However, when it comes to designing the autopilot, simplified models due to their simplicity and ease of implementation, have been exploited more frequently.

Non-linear models of UAVs based on Newton-Euler equations of motion have been derived by Blakelock [2], Brian, et. al. [3], Nelson [4], Roskam [5] McRuer [6]. Snell, et. al. [7], and Bugajski, et. al. [8] have considered six (6) DOF non-linear dynamics. Fifteen 1st order differential equations have been developed where the chosen states are position in Earth Fixed frame, three rates, attitude angles, longitudinal velocity, angle of attack and side slip angle. The aerodynamic coefficients needed to calculate the aerodynamic forces and moments are generally obtained by wind tunnel testing or CFD (Computational Fluid Dynamics) analysis.

Due to nonlinearities and coupling in equations of motion, no closed form solution exists and a steady state solution can only be computed using a numerical approach. Therefore, while designing flight control systems, researchers often simplify these equations. Simplification generally involves linearization and decoupling. However, the linearized equations of motion are valid only for small perturbation about the reference trim conditions. On the basis of assumption that the perturbed motion is small, the element of decoupling also kicks in. Following this approach, a Non-linear Fully-coupled aircraft model can be divided into two linear and decoupled sub-systems, i.e. one describing longitudinal dynamics and the other dealing with lateral motion.

The paper is divided into six main sections. Section 2 describes the assumptions for simplification of mathematical model. A complete nonlinear model is presented in Section 3. Section 4 is devoted to summarize the simulation results of this nonlinear model. Linearization of the model is described in Section 5. Section 6 concludes the paper by summarizing the discussion.

2. CONSIDERATIONS WHILE DERIVING MATHEMATICAL MODEL FOR UAV

While deriving the mathematical model of UAVs based on physical principles, complexities in the model can be significantly reduced by giving due considerations to the operational environment of UAVs such as physical dimensions, height ceiling and/or mission requirements. In particular, following assumptions are made for simplification of the mathematical model, as presented in [9]. These assumptions reduce the complexity of the mathematical model thus simplifying analysis and design problems without compromising accuracy.

(a) UAV is considered as a rigid body.

(b) Mass distribution is considered to be constant.

(c) Since the flight is mostly of short range and slow speed, earth's curvature and its rotation about its axis is ignored.

(d) UAVs fly at low speeds, hence the effects of flying at high Mach-Numbers is also neglected.

(e) Centripetal and Coriolis acceleration are neglected.

(f) UAVs mostly fly at the height of a few hundred meters above the ground level so it is legitimate to assume all altitude-dependent parameters to be constants. Thus, the same trimming condition will be applicable at different altitudes.

(g) Take off and landing is not considered so the angle of attack is considered to be small, i.e. small angle approximation is generally valid. It also implies that the aerodynamic forces and moments can be defined by the linear functions of aerodynamic angles, angular velocity and control surface deflections.

(h) The mass of the UAV remains constant during any particular dynamic analysis. So, the amount of fuel consumed during the period of dynamic analysis can be safely neglected since low powered engines have relatively lesser specific fuel consumption.

(i) Normally, most of the UAVs are designed to be axially symmetrical such that the moment generated by the control surface does not affect the direction of flight and the moment equations can be simplified by neglecting effects of the cross coupling inertia coefficients.

(j) Right handed system is used.

3. UAV MODEL

Modeling of UAV is being presented as a two step process. The set of dynamic equations describing UAV's flight profiles is presented first. In the second step, a method to dynamically compute the Engine Thrust, i.e. the main driving force for the UAV, is described. This set of dynamic model and Thrust computation method enables one to carryout meaningful and realistic simulations of the complete closed-loop system for evaluating the performance of various Autopilot controller designs.

3.1 Dynamic Equations Describing UAV Model

The set of dynamic equations representing UAV's mathematical model consists of 15 differential equations, i.e. three position equations, three velocity equations, three moment equations, three kinematic equations and three wind axis equations. These equations are summarized below, the relationship among various variables used in these equations is shown in Fig. 1.

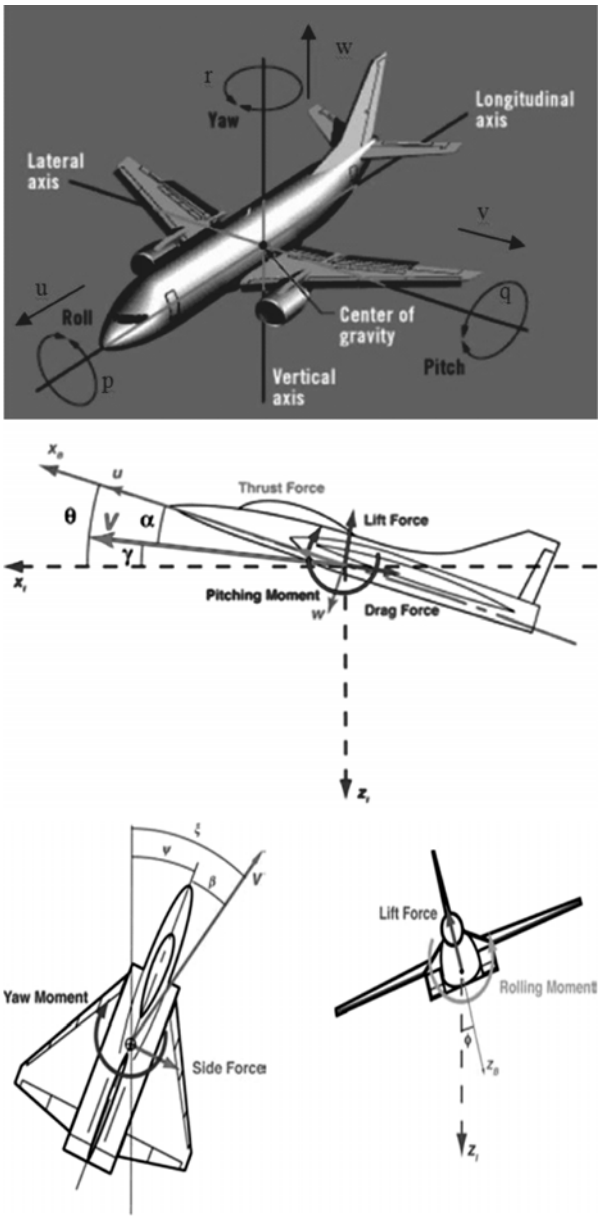

FIG. 1. ILLUSTRATION OF VARIABLES IN EOMS

3.1.1 Position Equations

$$\begin{aligned}\dot{X} &= u\cos\theta\cos\phi + v\left(-\cos\phi\sin\psi + \sin\theta\cos\psi\right) + \\ & w\left(\sin\phi\sin\psi + \cos\phi\sin\theta\cos\psi\right) \\ \dot{Y} &= u\cos\theta\sin\psi + v\left(\cos\phi\cos\psi + \sin\theta\sin\psi\right) + \\ & w\left(\sin\phi\cos\psi + \cos\phi\sin\theta\sin\psi\right) \\ \dot{Z} &= u\sin\theta - v\left(\sin\phi\cos\theta\sin\psi\right) - \omega\left(\cos\theta\cos\theta\right)\dot{h}\end{aligned} \tag{1}$$

3.1.2 Velocity Equations

$$\begin{aligned}\dot{u} &= rv - wq - g\sin\theta + \left(\frac{T + D\cos\alpha\cos\beta - L\sin\alpha - Y\cos\alpha\sin\beta}{M}\right) \\ \dot{v} &= -ru - wq - g\sin\phi\cos\theta + \left(\frac{D\sin\beta + Y\cos\beta}{M}\right) \\ \dot{w} &= ru - wq - g\sin\theta + \left(\frac{T + D\cos\alpha\cos\beta - L\sin\alpha - Y\cos\alpha\sin\beta}{M}\right)\end{aligned} \tag{2}$$

3.1.3 Moment Equations

$$\begin{aligned}\dot{p} &= \left[I_Z l + XI_{XZ} n + I_{XZ}\left(I_X - I_Z + I_Y\right)pq + \frac{\left(I_Z I_Y - I_Z^2 - I_{XZ}^2 qr\right)}{\left(I_X I_Z - I_{XZ}^2\right)}\right] \\ \dot{q} &- \left[m - pr\left(I_X - I_Z\right) - I_{XZ}\frac{\left(p^2 - r^2\right)}{\left(I_Y\right)}\right] \\ \dot{r} &= \left[I_{XZ} l + I_X n + \left(I_X^2 - I_Y I_X\right)pq - I_{XZ}\frac{\left(I_Z - I_Y + I_X\right)pr}{\left(I_X I_Z - I_{XZ}^2\right)}\right]\end{aligned} \tag{3}$$

3.1.4 Kinematic Equations

$$\begin{aligned}\dot{\phi} &= p + \tan\theta + q\sin\phi + r\cos\phi \\ \dot{\theta} &= q\cos\phi - r\sin\phi \\ \dot{\psi} &= \frac{\left(q\sin\phi + r\cos\phi\right)}{\cos\theta}\end{aligned} \tag{4}$$

3.1.5 Wind Axes Equations

$$\begin{aligned}\dot{V} &= \frac{\left(u\dot{u} - v\dot{v} + w\dot{w}\right)}{V} \\ \dot{\alpha} &= \frac{\left(u\dot{w} - w\dot{u}\right)}{\left(u^2 + w^2\right)} \\ \dot{\beta} &= (\dot{v}, V - v\dot{V}) / v^2\cos\beta\end{aligned} \tag{5}$$

Where, X, Y and Z are position components in geographical coordinate system, u, v and w are velocity components in body frame, θ, ϕ, ψ are attitude angles including pitch, roll and yaw respectively, h is altitude above sea level, p, q and r are rolling , pitching and yawing moments in body frame, α is angle of attack, β is sideslip angle, V is resultant velocity, T is the Engine Thrust, M is UAV mass, I_X, I_Y and I_Z are moments of inertia, and I_{XZ}, I_{XY} and I_{YZ} are the products of these inertia. D, L, Y are Drag, Lift and Side-Force, while 'l', 'm' and 'n' represent moments about x, y and z axes, respectively; and are computed using following relations:

$$\begin{aligned} D &= QSC_D & L &= QSC_L \\ Y &= QSC_Y & l &= QSbC_l \\ m &= QSCC_m & n &= QSbC_n \end{aligned} \tag{6}$$

Q represents dynamic pressure, S is the reference wing area, b describes reference wing span, and C is mean wing aerodynamic chord length. C_D, C_L, C_Y, C_l, C_m and C_n are drag, lift, side force and rolling , pitching and yawing moment coefficients respectively and are defined as:

$$\begin{aligned}C_D &= C_{DO} + C_D^{\alpha} + \frac{C_D^q Q\bar{C}}{2V} + \frac{C_D^{\dot{\alpha}}\dot{\alpha}\bar{C}}{2V} + \frac{C_D^u u}{v} + C_D^{\delta_e}\delta_e \\ C_Y &= C_Y^{\beta}\beta + \frac{C_Y^p pb}{2V} + \frac{C_Y^r rb}{2V} + C_Y^{\delta a}\delta_a + C_Y^{\delta r}\delta_r \\ C_L &= C_{LO} + C_L^{\alpha}\alpha + \frac{C_L^q Q\bar{C}}{2V} + \frac{C_L^{\dot{\alpha}}\dot{\alpha}\bar{C}}{2V} + C_L^{\delta_e}\delta_e \\ C_l &= C_l^{\beta}\beta + \frac{C_l^p pb}{2V} + \frac{C_l^r rb}{2V} + C_l^{\delta a}\delta_a + C_l^{\delta r}\delta_r \\ C_m &= C_{m0} + C_m^{\alpha}\alpha + \frac{C_m^q Q\bar{C}}{2V} + \frac{C_m^{\dot{\alpha}}\dot{\alpha}\bar{C}}{2V} + \frac{C_m^u u}{V} + C_m^{\delta_e}\delta_e \\ C_n &= C_n^{\beta}\beta\frac{C_n^p pb}{2V} + \frac{C_n^r rb}{2V} + C_n^{\delta a}\delta_a + C_n^{\delta r}\delta_r\end{aligned} \tag{7}$$

Where δ_a, δ_e, δ_r are aileron, elevator and rudder deflections, respectively. These deflections are measured in radians. The ailerons are the control surfaces which are physically located on wings and are responsible for controlling the roll motion, whereas the elevators and rudders are located in tail section and are responsible for pitching and yawing motion respectively. Wings and tail are attached with body of UAV (fuselage). Placement of control surfaces and other important parts of an aircraft are illustrated in Fig. 2. All other coefficients used in above equations are defined in Table 1.

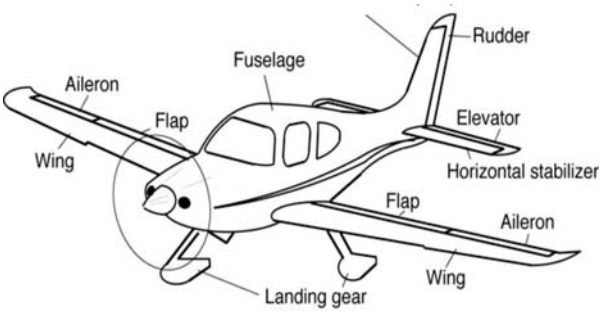

FIG. 2. IMPORTANT PARTS OF AIRFRAME

TABLE 1: DATA OF UAV

Symbol	Value	Description
C_{LO}	0.147	Coefficient of lift with zero angle of attack
C_L^{α}	4.54	Lift due to change in angle of attack
$C_L^{\dot{\alpha}}$	1.972	Lift due to change in rate of angle of attack
$C_L^{\delta e}$	0.37	Lift due to change in elevator deflection
C_L^{q}	5.54	Lift due to change in pitching moment
C_{DO}	0.0434	Zero drag
C_D^{u}	0.001	Coefficient of damping due to forward speed
$C_D^{\delta e}$	0.0	Drag due to change in ele vator deflection
C_Y^{β}	-0.83	Side force due to change in side slip angle
$C_Y^{\delta a}$	0.0	Side force due to change in aileron deflection
$C_Y^{\delta r}$	0.1914	Side force due to change in rudder deflection
C_Y^{p}	0.0085	Side force due to roll rate
C_Y^{r}	0.25	Side force due to yaw rate
C_{m0}	0.0001	Pitching moment with zero angle of attack
C_m^{α}	-0.39	Pitching moment due to change in alpha
C_m^{u}	0.0002	Pitching moment due to forward speed
$C_m^{\dot{\alpha}}$	-4.37	Pitching moment due to rate of alpha
$C_m^{\delta e}$	-1.2289	Pitching moment due to elevator deflection
C_m^{q}	-38.201	Pitching moment duc to q
C_l^{β}	-0.022	Roll moment due to side slip angle
$C_l^{\delta a}$	0.34	Roll moment due to aileron deflection
$C_l^{\delta r}$	0.0154	Roll moment due to rudder deflection
C_l^{p}	-0.3819	Roll moment due to p
C_l^{r}	0.0514	Roll moment due to r
C_n^{β}	0.1022	Yaw moment due to side slip angle
$C_n^{\delta a}$	-0.0088	Yaw moment due to aileron deflection
$C_n^{\delta r}$	-0.1404	Yaw moment due to rudder deflection
C_n^{p}	-0.017	Yaw moment due to p
C_n^{r}	-0.28	Yaw moment due to r
M	30	Mass of UAV (lbs)
S	10.9	Wing surface area (sq ft)
b	7.92	Wing span (ft)
$\bar{C}$	1.5	Mean chord length (ft)
I_X	1.08	Moment of inertia about X axis (slug-ft^2)
I_Y	2.01	Moment of inertia about Y axis (slug-ft^2)
I_Z	3.03	Moment of inertia about Z axis (slug-ft^2)
I_{XY}	0.0	Product of inertia XY axis (slug-ft^2)
I_{YZ}	0.0	Product of inertial YZ axis (slug-ft^2)
I_{XZ}	0.0	Product of inertia XZ axis (slug-ft^2)

3.2 Modeling of Engine Thrust

One of the major forces applied to UAV, as indicated in Equation (2) is the Engine Thrust. Although for simulation purposes, a fixed value of thrust is often used; however, in order to carryout realistic simulations of the complete closed-loop system which incorporates Autopilot designs, engine thrust computation has to be dynamic. Engine thrust is a function of rotational speed, diameter and thrust-coefficient of the propeller, and is given by:

$$T=\rho_r^{\,2}\, d^4\, C_T \tag{8}$$

Where ρ is the air density at current altitude; r, d and C_T represent the rotational speed, diameter and thrust-coefficient of the propeller, respectively.

Thrust coefficient (C_T) is a function of Advanced Ratio (J), which is a dimensionless term defined as a function of forward speed (V), rotational speed (r) of the propeller in RPM (Revolutions Per Second), and diameter (d) [9].

$$T = \frac{V}{\left(r \times d\right)} \tag{9}$$

Generally (C_T) data is available from propeller manufacturer in the form of graph as shown in Fig. 3.

Thrust coefficient curves depend mainly on propeller diameter, airfoil and pitch angle. Curves shown in Fig. 3 correspond to different "pitch to diameter p/d" ratio. In our case a 26x13" (dia x pitch) propeller is used with makes p/d ratio equals to 0.5. For simulation purposes, data shown in Fig. 3 is stored in the form of a lookup table, which is used to obtain (C_T) corresponding to a specific value of Advanced Ratio (J).

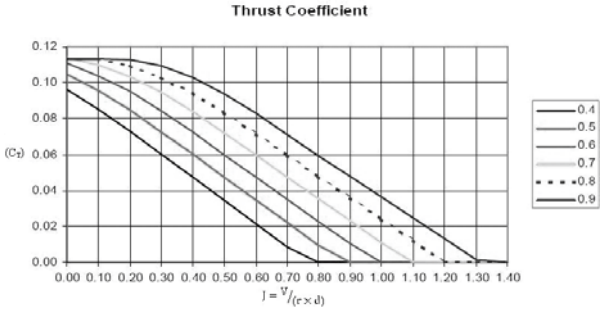

FIG. 3. THRUST COEFFICIENT VS ADVANCE RATIO

Another lookup table is prepared to give engine RPM values for different values of throttle input. This table is used to obtain RPMs corresponding to the commanded throttle input δ_T , which is then used to compute Advance Ratio (J) using Equation (9); the corresponding value of (C_T) is then obtained from C_T-vs- J lookup table, which in turn gives the Engine Thrust (T) using Equation (8). Values for the air density ρ at a specific altitude can be obtained from the atmosphere model. The 1976 COESA (Committee on Extension to the Standard Atmosphere) Model is often used for obtaining atmospheric data during simulations. The COESA model is available in MATLAB/Simulink's Aerospace Block Set [10] and the same has been used for the simulation of non-linear model in this paper.

4. IMPLEMENTATION OF NON-LINEAR MODEL

A small UAV has been selected for simulation and implementation of the Non-linear model presented in this paper. The geometric data and aerodynamic coefficients of this UAV used in simulations are listed in Table 1.

Block diagram of the Simulink model used for the implementation of the Non-linear UAV model is shown in Figure 4. The inputs to the system are δ_a, δ_e, δ_r and δ_T representing deflections of ailerons, elevators, rudders and the throttle input, respectively. Fifteen states of the model include three angular velocities, three translational velocities, geographical position, attitude angles, angle of attack and side slip angle.

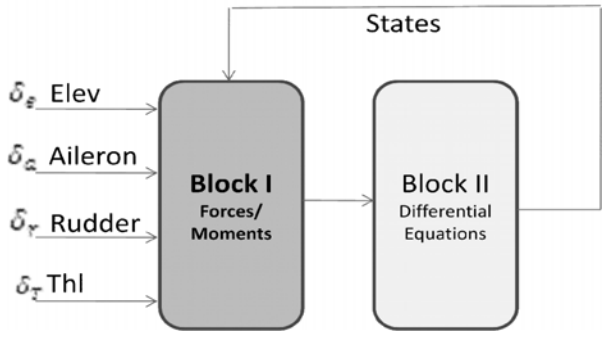

FIG. 4. BLOCK DIAGRAM OF NON-LINEAR MODEL

Block-I calculates the aerodynamic forces, moments and engine thrust using Equations (6-9), whereas Block-II solves the differential Equations (1-5) and outputs fifteen states mentioned above. Simulation was run with zero initial conditions except longitudinal velocity (u0) 36 m/s, altitude (h) 500 m., zero input to aileron and rudder, sixty percent throttle and a unit-step for elevator. Open loop results are presented in Fig. 5.

In response to a Step command for elevator input, an increase in pitch angle is observed. Due to pitch up attitude, decrease in velocity and increase in altitude can also be noted. In the absence of a roll-controller, coupling effect introduced a roll angle, which contributes towards introducing negative pitch angle; as a result UAV eventually attains a nose down attitude which can be seen after approximately 15 seconds in Fig. 5.

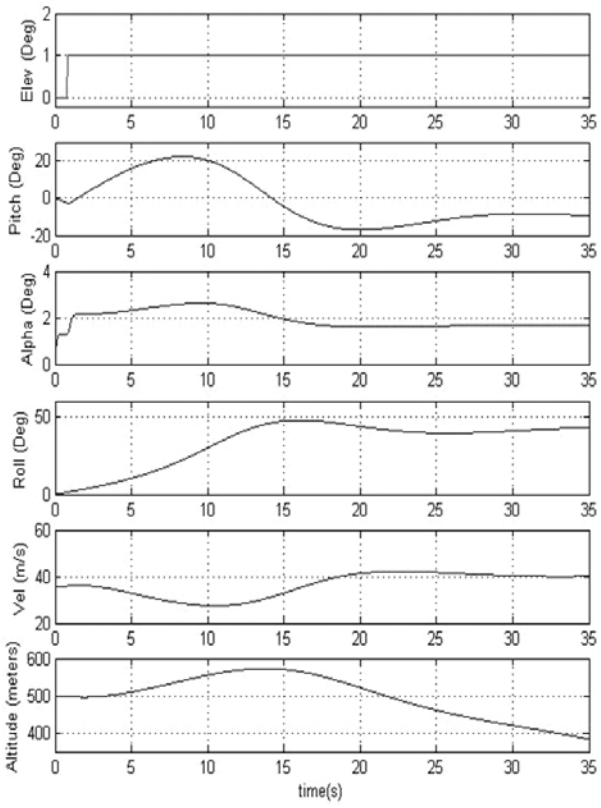

FIG. 5. OPEN LOOP RESPONSE OF NON LINEAR MODEL

5. LINEARIZATION

In order to design controller for a Non-linear system, linearization of the plant model about some equilibrium point is often used to simplify the design process. Different linearization techniques are described in literature; we have chosen the method presented in [5] to develop the State-Space model for the longitudinal and lateral modes of UAV. The resulting longitudinal model with elevator input and lateral model with aileron and rudder inputs are presented in Equations (10-11), respectively.

$$\begin{bmatrix} \Delta\dot{u} \\ \Delta\dot{\alpha} \\ \Delta\dot{q} \\ \Delta\dot{\theta} \\ \Delta\dot{h} \end{bmatrix} = \begin{bmatrix} X_u & X_\alpha & 0 & -g & 0 \\ \frac{Z_u}{u_0 - Z_{\dot{\alpha}}} & \frac{Z_\alpha}{u_0 - Z_{\dot{\alpha}}} & \frac{u_0}{u_0 - Z_{\dot{\alpha}}} & 0 & 0 \\ M_u & M_\alpha & M_q & 0 & 0 \\ 0 & 0 & 1 & 0 & 0 \\ 0 & -u_0 & 0 & u_0 & 0 \end{bmatrix} \begin{bmatrix} \Delta u \\ \Delta\alpha \\ \Delta q \\ \Delta\theta \\ \Delta h \end{bmatrix} + \begin{bmatrix} X_{\delta e} \\ Z_{\delta e} \\ M_{\delta e} \\ 0 \\ 0 \end{bmatrix} \begin{bmatrix} \Delta\delta e \end{bmatrix} \quad (10).$$

$$\begin{bmatrix} \Delta\dot{p} \\ \Delta\dot{\phi} \\ \Delta\dot{\beta} \\ \Delta\dot{r} \\ \Delta\dot{\psi} \end{bmatrix} = \begin{bmatrix} L_p & 0 & L_\beta & L_r & 0 \\ 1 & 0 & 0 & 0 & 0 \\ \frac{Y_p}{u_0} & \frac{g\cos\theta}{u_0} & \frac{Y_\beta}{u_0} & \frac{Y_r - u_0}{u_0} & 0 \\ N_p & 0 & N_\beta & N_r & 0 \\ 0 & 0 & 0 & 1 & 0 \end{bmatrix} \begin{bmatrix} p \\ \phi \\ \beta \\ r \\ \psi \end{bmatrix} + \begin{bmatrix} L_{\delta a} & L_{\delta r} \\ 0 & 0 \\ Y_{\delta a} & Y_{\delta r} \\ N_{\delta a} & N_{\delta r} \\ 0 & 0 \end{bmatrix} \begin{bmatrix} \Delta\delta_a \\ \Delta\delta_r \end{bmatrix} \begin{bmatrix} L_{\delta a} & L_{\delta r} \\ 0 & 0 \\ Y_{\delta a} & Y_{\delta r} \\ N_{\delta a} & N_{\delta r} \\ 0 & 0 \end{bmatrix} \begin{bmatrix} \Delta\delta_a \\ \Delta\delta_r \end{bmatrix} \quad (11)$$

Substituting the values of dimensional derivatives in Equation (10) and neglecting altitude for the time being, following longitudinal model is obtained:

$$\begin{bmatrix} \Delta\dot{u} \\ \Delta\dot{\alpha} \\ \Delta\dot{q} \\ \Delta\dot{\theta} \end{bmatrix} = \begin{bmatrix} -0.23 & 12.45 & 0 & -9.8 \\ -0.004 & -7.81 & 0.92 & 0 \\ 0.016 & 9.18 & -15.14 & 0 \\ 0 & 0 & 1 & 0 \end{bmatrix} \begin{bmatrix} u \\ \alpha \\ q \\ \theta \end{bmatrix} + \begin{bmatrix} 0 \\ -0.01 \\ -2.59 \\ 0 \end{bmatrix} \begin{bmatrix} \Delta\delta e \end{bmatrix} \quad (12)$$

Similarly, by substituting the dimensional derivatives in Equation (11), following lateral model is obtained

$$\begin{bmatrix} \Delta\dot{p} \\ \Delta\dot{\phi} \\ \Delta\dot{\beta} \\ \Delta\dot{\gamma} \end{bmatrix} = \begin{bmatrix} -25.61 & 0 & -28.36 & 3.24 \\ 1.0 & 0 & 0 & 0 \\ 0.0011 & 0.2723 & -0.47 & -0.98 \\ -0.60 & 0 & 46.95 & -4.52 \end{bmatrix} \begin{bmatrix} p \\ \phi \\ \beta \\ \gamma \end{bmatrix} + \begin{bmatrix} 482 & 28.5 \\ 0 & 0 \\ 0 & 0.38 \\ 4.10 & -46.76 \end{bmatrix} \begin{bmatrix} \Delta\delta a \\ \Delta\delta\gamma \end{bmatrix} \quad (13)$$

Dimensional stability derivatives shown in Equation (10) for longitudinal model and Equation (11) for lateral models are calculated using equations listed in Table 2.

Eigen-value analysis of longitudinal model Equation (12) reveals the dynamic characteristics of the sub-system, which are given in Table 3.

TABLE 2: FORMULAE FOR CALCULATION OF STABILITY DERIVATIVES

Longitudinal Derivatives	Lateral Derivatives
$X_U = -QS(C_D^U + 2C_{D0})/Mu_0$	$L_p = QSb^2C_l^p/2I_X u_0$
$Z_U = -QS(C_L^U + 2C_{L0})/Mu_0$	$L_\beta = QSC_l^\beta/I_X$
$Z_\alpha = -QS(C_L^\alpha + 2C_{D0})/M$	$L_r = QSb^2C_l^r/2I_X u_0$
$M_U = QSC(C_m^u + 2C_{m0})/I_Y u_0$	$L_{\delta a} = QSbC_l^{\delta a}/I_X$
$M_\alpha = QSC(C_m^\alpha)/I_Y$	$L_{\delta r} = QSbC_l^{\delta r}/I_X$
$M_q = QSCC(C_m^q)/2I_Y u_0$	$Y_p = QSbC_Y^p/2Mu_0$
$X_{\delta e} = -QS(C_D^{\delta e})/M$	$Y_\beta = QSC_Y^\beta/M$
$Z_{\delta e} = -QS(C_L^{\delta e})/m$	$Y_r = QSbC_Y^r/2Mu_0$
$M_{\delta e} = QSC(C_m^{\delta e})/I_Y$	$Y_{\delta a} = QSC_Y^{\delta a}/M$
$Z_\alpha = -QSC(C_L^\alpha)/2Mu_0$	$Y_{\delta r} = QSC_Y^{\delta r}/M$
	$N_p = QSb^2C_n^p/2I_Z u_0$
	$N_\beta = QSbC_n^\beta/I_Z$
	$N_r = QSb^2C_n^r/2I_Z u_0$
	$N_{\delta a} = QSbC_n^{\delta a}/I_Z$
	$N_{\delta r} = QSbC_n^{\delta r}/I_Z$

This analysis reveals that the UAV under consideration has two pairs of complex conjugate roots for its longitudinal dynamics. Both the modes, i.e. Phugoid and Short Period exhibit highly damped response.

The dynamic characteristics of lateral system Equation (13) are given in the Table 4.

The results show a typical lateral dynamic response for the UAV characterized by a very fast roll mode, a low damped Dutch roll mode and an unstable spiral mode.

6. CONCLUSION

In model based control design techniques, the significance of a realistic mathematical model of the plant cannot be undermined. An endeavor is made to gather all the related concepts and mathematical equations, and present the consolidated dynamic model of a UAV along with all the required data for a real UAV. This would enable researchers to use the developed model and carry out realistic simulations of controllers/ autopilots.

TABLE 3. DYNAMIC CHARACTERISTICS OF LONGITUDINAL MODE

Eigen Value	Damping Ratio	Frequency (rad/sec)	Period (sec)	Mode
-.118±.187i	0.53	0.221	28.41	Phugoid
-11.5±2.08i	0.98	11.7	0.536	Short Period

TABLE 4. DYNAMIC CHARACTERISTICS OF LATERAL MODE

Eigen Value	Damping Ratio	Frequency (rad/sec)	Period (sec)	Mode
.004	1.0	-	-	Spiral
-25.6	1.0	-	-	Roll
-2.52±6.57i	0.35	7.04	0.89	Dutch Roll

ACKNOWLEDGEMENT

Authors would like to express our gratitude to all those who gave us the possibility to complete this paper. Authors also thankful to Mehran University of Engineering & Technology, Jamshoro.

REFERENCES

[1] Sadraey, M., and Colgren, R., "UAV Flight Simulation: Credibility of Linear Decoupled vs Nonlinear Coupled Equations of Motion", AIAA Modeling and Simulation Technologies Conference and Exhibit, pp 15-18 California, August, 2005.

[2] John, H., "Blakelock, Automatic Control of Aircraft and Missiles", John Willy and Sons, USA.

[3] Brian, L.S., and Frank, L.L., "Aircraft Control and Simulation", John Willy and Sons, USA.

[4] Robert, C.N., "Flight Stability and Automatic Control", McGraw-Hill Book Company, USA.

[5] Jan, R., "Airplane Flight Dynamics and Automatic Flight Control", Roskam Aviation and Engineering Corporation, USA.

[6] McRuar, D., "Aircraft Dynamics and Automatic Control", Princeton University Press, New Jersey, USA.

[7] Snell, S.A., Enns, D.F., and Garrad, W.L., "Nonlinear Inversion Flight Control for a Super-Maneuverable Aircraft", Journal of Guidance, Control and Dynamics, Volume 15, No. 4, July-August, 1992.

[8] Bugajski, D.J., and Enns, D.F., "Nonlinear Control Law with Application to High Angle of Attack Flight", Journal of Guidance, Control and Dynamics, Volume 15 No. 3, May-June, 1992.

[9] Huo, I.L., "Development of a Pilot Training Platform for UAVs Using a 6DOF Nonlinear Model with Flight Test Validation", AIAA Modeling and Simulation Technologies Conference, Hawaii, 2008

[10] Aerosim Block Set, available at http://www,u-dynamics.com